Available online at www.sciencedirect.com

jmr&t Journal of Materials Research and Technology

www.jmrt.com.br

Short Communication

Tensile behaviour of aluminium 7017 alloy at various temperatures and strain rates

*Ravindranadh Bobbili**, *Vemuri Madhu*, *Ashok Kumar Gogia*

Defence Metallurgical Research Laboratory, Hyderabad, India

ARTICLE INFO

Article history:
Received 2 May 2015
Accepted 7 December 2015
Available online 21 January 2016

Keywords:
Aluminium 7017
J-C model
Strain rate

ABSTRACT

The objective of the present study is to carry out high strain rate tensile tests on 7017 aluminium alloy under different strain rates ranging from 0.01, 500, 1000 and 1500 s^{-1} and at temperatures of 25, 100, 200 and 300 °C. Quasi-Static tensile stress–strain curves were generated using INSTRON 8500 machine. Johnson-Cook (J-C) constitutive model was developed for 7017 aluminium alloy based on high strain rate tensile data generated from split Hopkinson tension bar (SHTB) at various temperatures. This study evidently showed an improvement in dynamic strength as the strain rate increases. The predictions of J-C model are observed to be in consistence with the experimental data for all strain rates and temperatures. The fracture surfaces of specimens tested were studied under SEM. The change in fracture mode has been observed at different strain rates. The shear mode of fracture is dominant at lower strain rates (0.01 and 500 s^{-1}); whereas cup- and cone-like surface representing dimple structure is found at the higher strain rates (1000 and 1500 s^{-1}). The numbers of dimples at high strain rates are more than the quasi-static and intermediate strain rates. It is also observed that the flow stress decreases with increase in temperature. The 7017 aluminium alloy demonstrates thermal softening at higher temperatures. So when the temperature is more than 200 °C at these strain rates, thermal softening is predominant mode of deformation mechanism. It is found that when the temperature increases to 200 °C, the number of dimples rises and the dimple size of 7017 aluminium alloy is larger than at lower temperatures.

1. Introduction

Aluminium alloys are widely employed in the automobile and armour applications to enhance crashworthiness and reduce weight of the components. The understanding of the strain rate sensitivity parameters and mechanism of deformation of these alloys is indispensable for the successful design of components. Aluminium alloys have found potential applications due to high strength to density ratio. Al 7017 alloy has got uses in armour applications. Many ballistic experiments were carried out on this alloy against 7.62AP projectiles in normal and oblique configurations [1,2]. Hence, it is important to investigate the material deformation characteristics under high

* *Corresponding author.*
E-mail: ravindranadhb@gmail.com (R. Bobbili).
http://dx.doi.org/10.1016/j.jmrt.2015.12.002

strain rate loading conditions. The data obtained will be helpful for incorporating in constitutive strength models. In order to develop more robust strength models and failure criteria under dynamic loading tensile and compression experimental data performed over wide range of strain rates is necessary [3,4].

The effect of strain rate on properties viz. flow stress, strain rate sensitivity, etc., varies for each material. High strain rate compressive deformation behaviour of AA 6082 and AA 7108 alloy under peak tempered and overaged condition shows low strain rate sensitivity. Also a trend of negative strain rate sensitivity was observed at strain rates higher than 2000 s^{-1} [5]. Smerd et al., have shown marked increase in elongation with increase in strain rate [6]. Similar increase in ductility has also been reported in Al 7075 alloy by El Magd et al. [7]. Metallographic investigations of the material showed ductile shear failure. Existence of two regions of strain rate sensitivity in Al 7075 over a range of strain rates has been explained by Lee et al. [8]. It has been reported that in the strain rate regime of 10^2–10^3 s^{-1}, the strain rate has only slight effect on flow stress, whereas at strain rates higher than 10^3 s^{-1}, the flow stress increases more rapidly with strain rate having an approximate linear relationship.

Lin et al. [9] studied the compressive behaviour of aluminium 2124-T851 alloy under the strain rates of 0.01–10 s^{-1} and temperature range of 653–743 °C. A modified constitutive model accommodating the effects of material behaviour was proposed.

Haghdadi et al. [10] predicted the high temperature flow behaviour of a cast A356 aluminium alloy to optimize the design of forming process. An artificial neural network (ANN) was adopted to determine the flow stress characteristics under different loading conditions. A series of isothermal compression tests was performed in the temperature range of 400–540 °C and strain rates of 0.001–0.1 s^{-1}. Lee et al. [11] investigated the high temperature impact properties and microstructural evolution of 6061-T6 aluminium alloy at temperatures ranging from 100 to 350 °C and strain rates ranging from 1000 to 5000 s^{-1} using a compressive split-Hopkinson pressure bar (SHPB) system. The experimental results revealed that the flow stress and strain rate sensitivity increased with increasing strain rate or decreasing temperature. The flow stress–strain response of the 6061-T6 alloy was effectively described by the Zerilli–Armstrong fcc model. Pérez-Bergquist et al. [12] studied the mechanical response of aluminium alloys 5083, 5059 and 7039 in compression and shear, in both the quasi-static (0.001 s^{-1}) and dynamic (2000 s^{-1}) strain rate regimes. The mechanical responses in shear were found to be strain-rate sensitive. To evaluate the thermo mechanical response of these alloys, both dynamic and quasi-static tests were performed at temperatures ranging from 20 to 300 °C. The 7039 alloy exhibited the highest strength in compression at room temperature followed by alloys 5059 and 5083 respectively.

So far no attempt has been made to study the effect of strain rate and temperature on dynamic tensile flow stress of 7017 aluminium alloy. The objective of the present study is to develop constitutive models for predicting the dynamic tensile flow stress of 7017 aluminium alloy during high strain rate deformation. The fracture surfaces of specimens tested under various strain rates and temperatures were studied by under SEM.

Fig. 1 – Photo of the quasi static tensile specimen of aluminium 7017 alloy.

2. Experimental methods

2.1. Materials and test setup

The present alloy under study is Al–4.5Zn–2.5Mg–0.3Si–0.40Fe, commercially named as 7017 aluminium alloy (peak aged). Tensile testing was performed at various temperatures on tensile specimens (Fig. 1) using INSTRON 8500 testing machine at a crosshead speed of 1.0 mm/min. Specimens have been tested according to ASTM E8 M11 standard in a temperature range between 20 and 300 °C, at strain rate of 0.01 s^{-1}. Three specimens were tested at each set of conditions. The quasi static yield and ultimate tensile strengths of the alloy are 458 MPa and 508 MPa, respectively. Ductility measured as percentage elongation is 13%. The authors have also performed high strain rate compression tests of various strain rates at room temperature.

High strain rate tensile testing of 7017 aluminium alloy samples of length 45 mm and diameter 10 mm (ASTM E8) was carried out using SHTB apparatus. Fig. 2 shows the SHTB equipment with heating system, specification of the specimen used and arrangement for testing. The resistance wire heating method is used to elevated temperature dynamic experiment. The specimens are heated by the resistance-heated furnace. Thermocouple wire is connected on the specimen, which can measure the specimen temperature variation. Fig. 3 shows the tensile fractured specimens at different strain rates and temperatures.

The pressure wave was generated by impacting a striker bar (projectile) to input (incident) pressure bar. The striker bar was propelled by a gas gun system attached at one end. The strain gages in conjunction with amplifiers and associated instrumentation record these wave pulses. Since the specimen deforms uniformly, the strain rate within the specimen are directly proportional to the amplitude of the reflected wave (ε_r).

Strain-rate generated in the specimen

$$\dot{\varepsilon} = \frac{-2c\varepsilon_r}{l} \quad (1)$$

Hence strain in the specimen is

$$\varepsilon = \frac{-2c}{l\int_0^t \varepsilon_r dt} \quad (2)$$

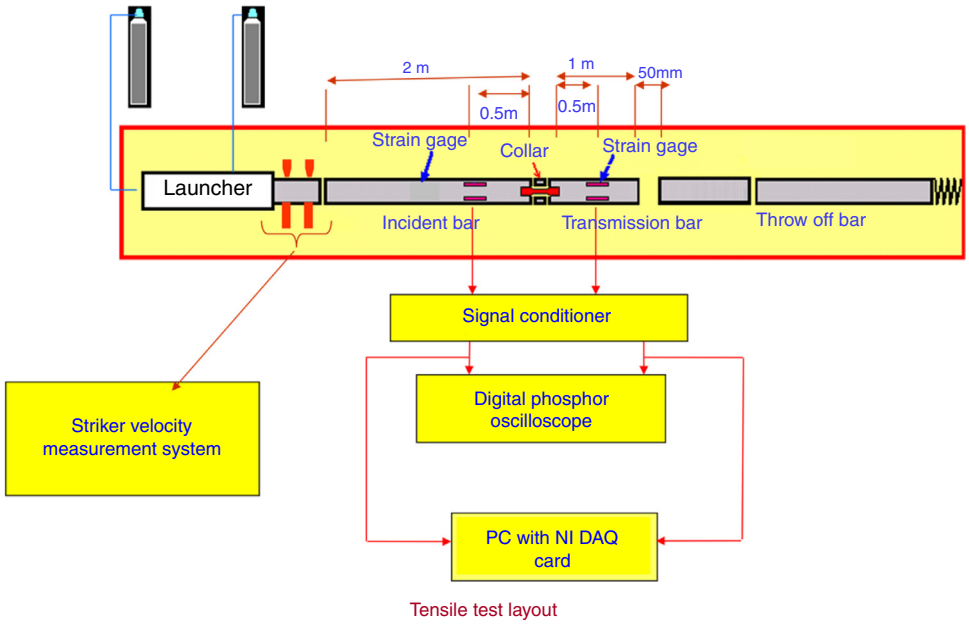

Fig. 2 – Schematic diagram of Split Hopkinson tension bar (SHTB).

Stress in the specimen can be calculated as

$$\sigma = \frac{AE\varepsilon_t}{A_S} \tag{3}$$

where A and A_S are the area of the bar and specimen respectively, l is length of the specimen, c is wave speed, ε_t is the strain in the transmitted bar and E is the elastic modulus of the pressure bar.

2.2. *Johnson-Cook model*

High-strain rate plastic deformation of materials can be described by various constitutive equations that basically attempt to address dependence of stress on strain, strain rate and temperature. In this regard, stress can be schematically presented as

$$\sigma = f(\varepsilon, \dot{\varepsilon}, T) \tag{4}$$

There are a number of equations that have been proposed to describe the plastic behaviour of materials as a function of strain rate and temperature. At low strain rates, metals are known to work harden along the well known relationship known as parabolic hardening and expressed as $\sigma = \sigma_o + k\,\varepsilon^n$.

Here σ_o is the yield stress, n is work hardening exponent and k is pre-exponential factor.

The effect of strain rate on strength [13,14] is generally expressed as: $\sigma \propto \ln \dot{\varepsilon}$

But the above relationship breaks down at strain rate above $10^2\,s^{-1}$.

The effects of temperature on the flow stress can be represented by:

$$\sigma = \sigma_r \left[1 - \left(\frac{T - T_r}{T_m - T_r}\right)^m\right] \tag{5}$$

Here T_m is the melting temperature; T_r is the reference temperature at which σ_r is the reference stress.

The dynamic flow stress depicting effect of various parameters has been expressed by Johnson-Cook model [15,16] as

$$\sigma = (A + B\varepsilon^n)(1 + C\,\ln\,\dot{\varepsilon}^*)(1 - T^{*m}) \tag{6}$$

where A is the yield stress, B and n represent the effect of strain hardening, C is the strain rate constant, ε is the equivalent plastic strain, $\dot{\varepsilon}$ is the strain rate, $\dot{\varepsilon}^*$ is the dimensionless plastic strain rate represented as $\dot{\varepsilon}/\dot{\varepsilon}_o$ for $\dot{\varepsilon}_o = 1\,s^{-1}$, T^* is the homologous temperature referred as $(T - T_{room})/(T_{melt} - T_{room})$, and m is the thermal softening factor. Thus, the term present in first, second and third bracket in Eq. (4) represents strain, strain rate and temperature effect, respectively. The J-C model is independent of pressure.

3. Results and discussion

A decrease of stress beyond a maximum stress at higher strain rate (Fig. 4) has been observed. This can be attributed to dominance of thermal softening. The deformation of the material under high strain rate loading being an adiabatic process means heat generated during the deformation process has insufficient time to dissipate before the deformation process is complete. This leads to conversion of a significant portion of the plastic work into heat and localization. The relation between plastic work and converted heat can be written as:

$$\eta \Delta W = \Delta Q \tag{7}$$

Here ΔW is equal to $\int \sigma\varepsilon$ and ΔQ is $C\rho\Delta T$, where, ρ is the density of the material undergoing deformation, C is specific heat

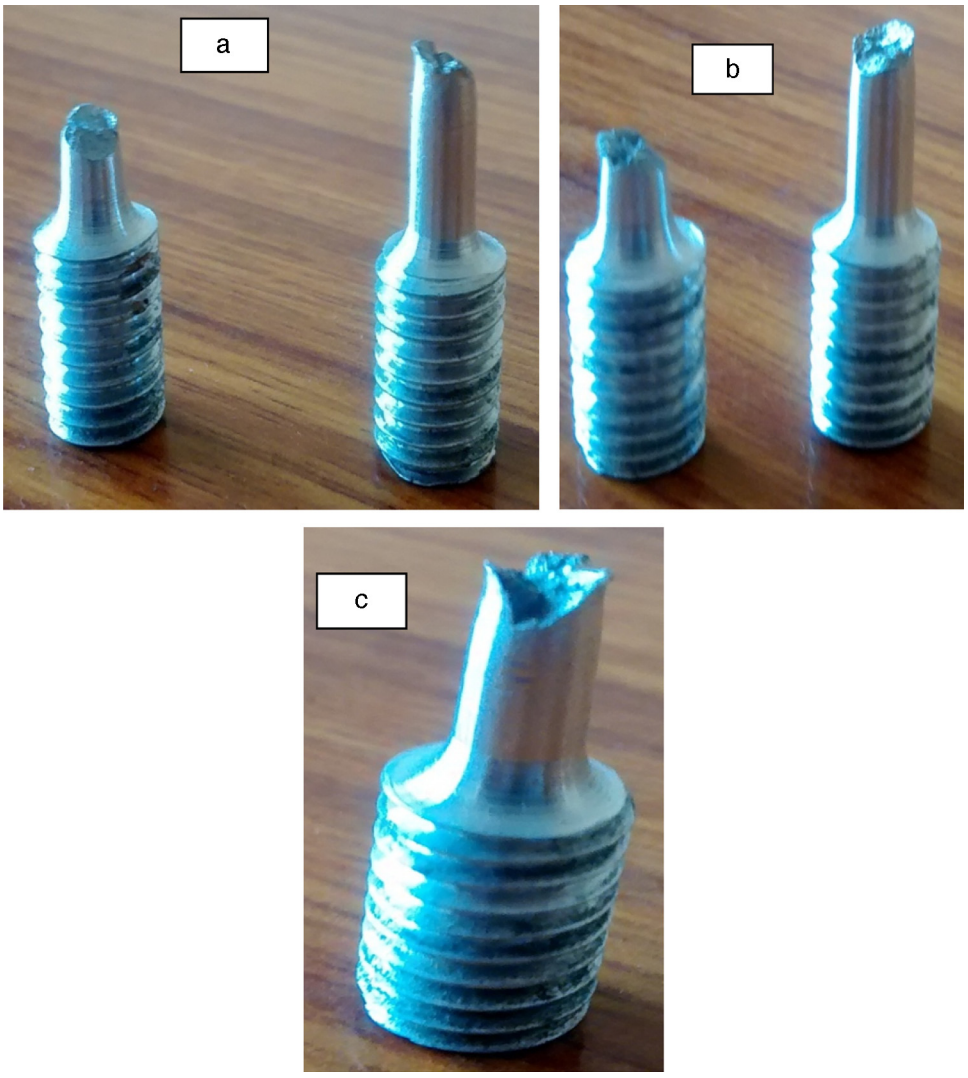

Fig. 3 – The photographs of fracture specimens of aluminium 7017 alloy at strain rates of (a) 500/s, 100 °C; (b) 1500/s, 25 °C; (c) 500/s, 100 °C; (d) 2000/s, 25 °C.

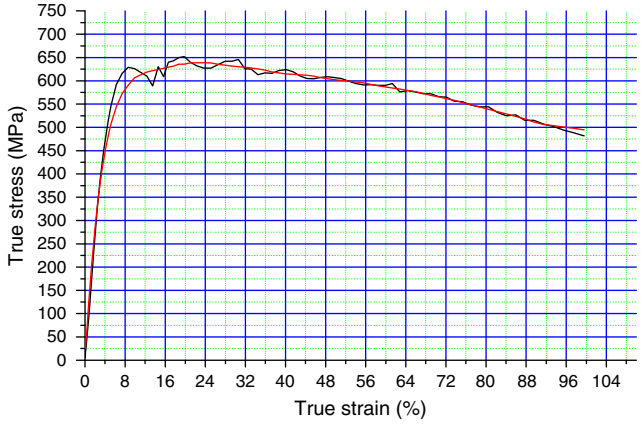

Fig. 4 – True stress–strain curves of Al 7017 alloy tested at 5500/s strain rate.

and ΔT is the value of temperature rise. Hence from Eq. (7), the value of temperature rise can be written as:

$$\Delta T = \frac{\eta \int \sigma \varepsilon}{C\rho} \tag{8}$$

Assuming 100% of the plastic work converts into heat ($\eta = 1.0$), and calculating area under the curve for a strain rate of 5500 s^{-1}, the temperature rise for aluminium 7017 alloy ($\rho = 2.8$ g/cc, $c = 950$ J/kg K) is calculated to be 254 °C. Similar behaviour was observed in Al 7075 alloy also [8]. That is why the deforming temperatures have been chosen from room temperature (25 °C) to 300 °C for this study.

At reference strain rate and reference temperature, the functions of strain rate hardening and thermal softening is equal to unity, J-C model [15] is simplified as follows:

$$\sigma = A + B\varepsilon^n \tag{9}$$

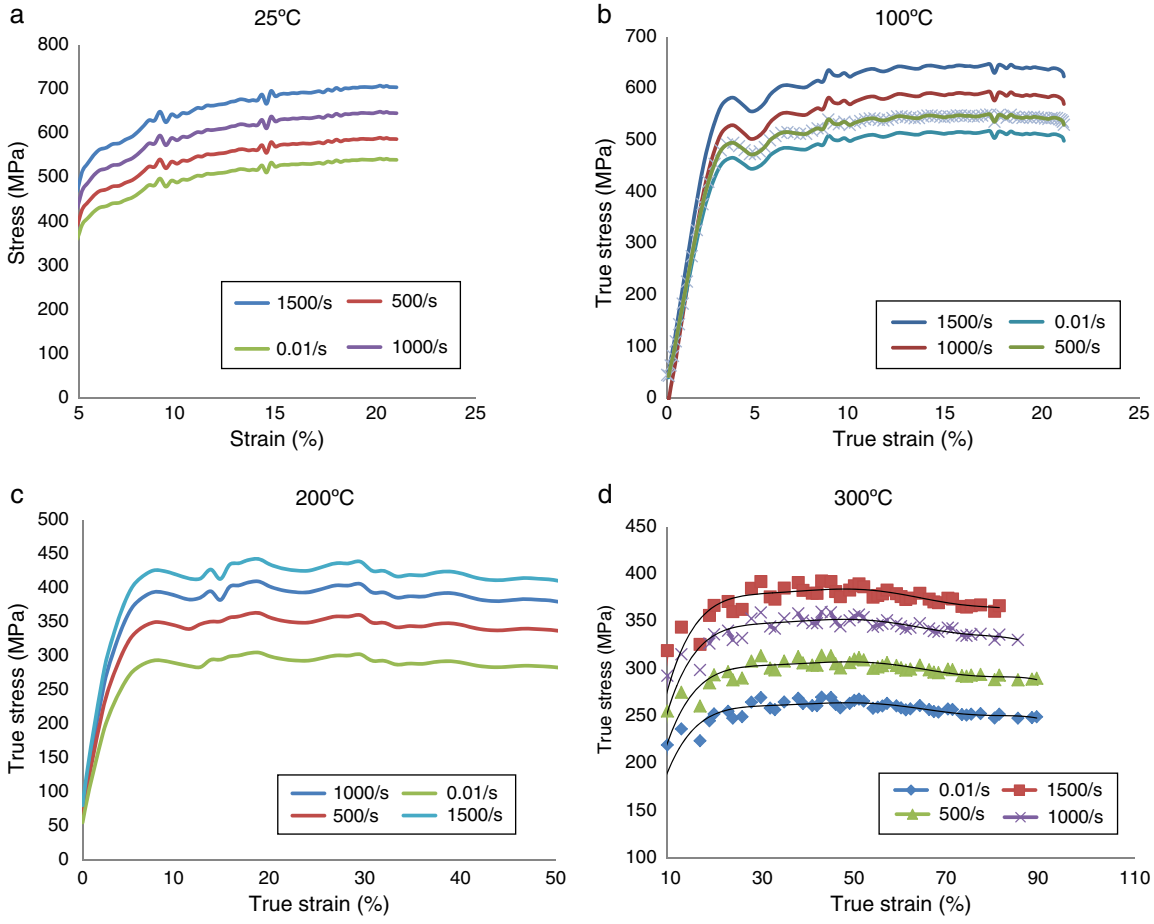

Fig. 5 – The stress strain curves of aluminium 7017 alloy at various temperatures of (a) 25 °C, (b) 100 °C, (c) 200 °C, and (d) 300 °C.

A is the yield stress (MPa) which can be directly obtained from observing the strain–stress curve. Plotting a line between $\ln \varepsilon$ and $\ln(\sigma - A)$ at the reference strain rate and reference temperature gives B (MPa) and n in Eq. (7). Strain rate sensitivity (m) is determined as the slope of linear fit of log (strain rate) vs dynamic flow stress/static stress using high strain rate data corresponds to a strain of 10%. The above constants are provided in Table 1.

The experimental data (Fig. 5) obtained from the high strain rate tensile tests on split Hopkinson tension bar, in a wide range of temperatures (25–300 °C) and strain rates (0.01–1500 s^{-1}), were employed to develop J-C model for 7017 aluminium alloy. Fig. 6 depicts the comparison of the experimental results with the predicted values at various strain rates and temperatures based on J-C strength model. It was noticed that the J-C model could predict the experimental data only

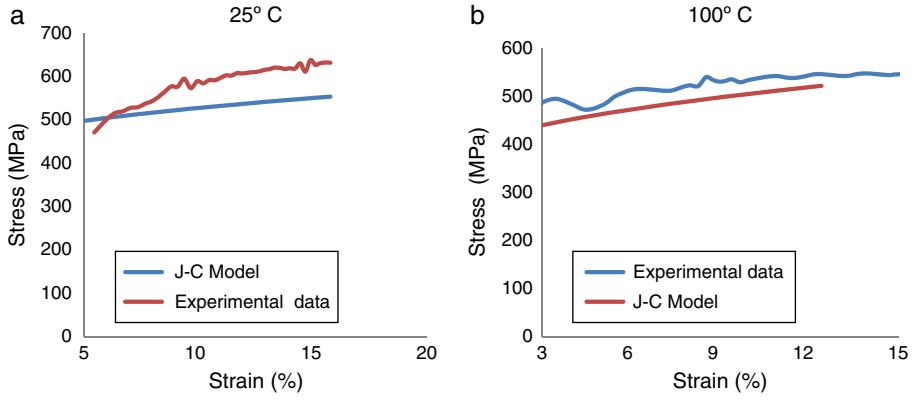

Fig. 6 – Comparison between J-C Model and experimental flow stress of aluminium 7017 alloy at strain rate of 500/s and temperatures of (a) 25 °C and (b) 100 °C.

Table 1 – Johnson-Cook Model constants for Al 7017 alloy.

A (MPa)	B (MPa)	N	C	M
410	528	0.5	0.0048	0.9

in the intermediate temperature range. This variation may be attributed to the error introduced by the fitting of the material constants at some conditions.

Tensile flow stress increases considerably from the strain rate of 0.01–1500 s^{-1}. The maximum tensile flow stress of 7017 aluminium alloy enhances by 250 MPa as the strain rate is increased from 0.01 to 1500 s^{-1} (Fig. 5). In order to describe the mechanism of failures under different loading conditions, the failure modes are investigated. Decreasing temperature and increasing strain rate can result in the increase of flow stress. This is because the low strain rate provides long time for energy accumulation, and high forming temperature promotes the nucleation and growth of dynamically recrystallized grains and dislocation annihilation, and thus reduces the stress level [16]. During the tensile tests, the strength of 7017 aluminium alloy is mainly dependent on deformation processes of strain hardening and thermal softening [17]. When the material undergoes plastic deformation, the dislocation density increases and causes the strain hardening. The change in fracture mode has been observed at different strain rate loading conditions. A shear mode (Fig. 3) of fracture is

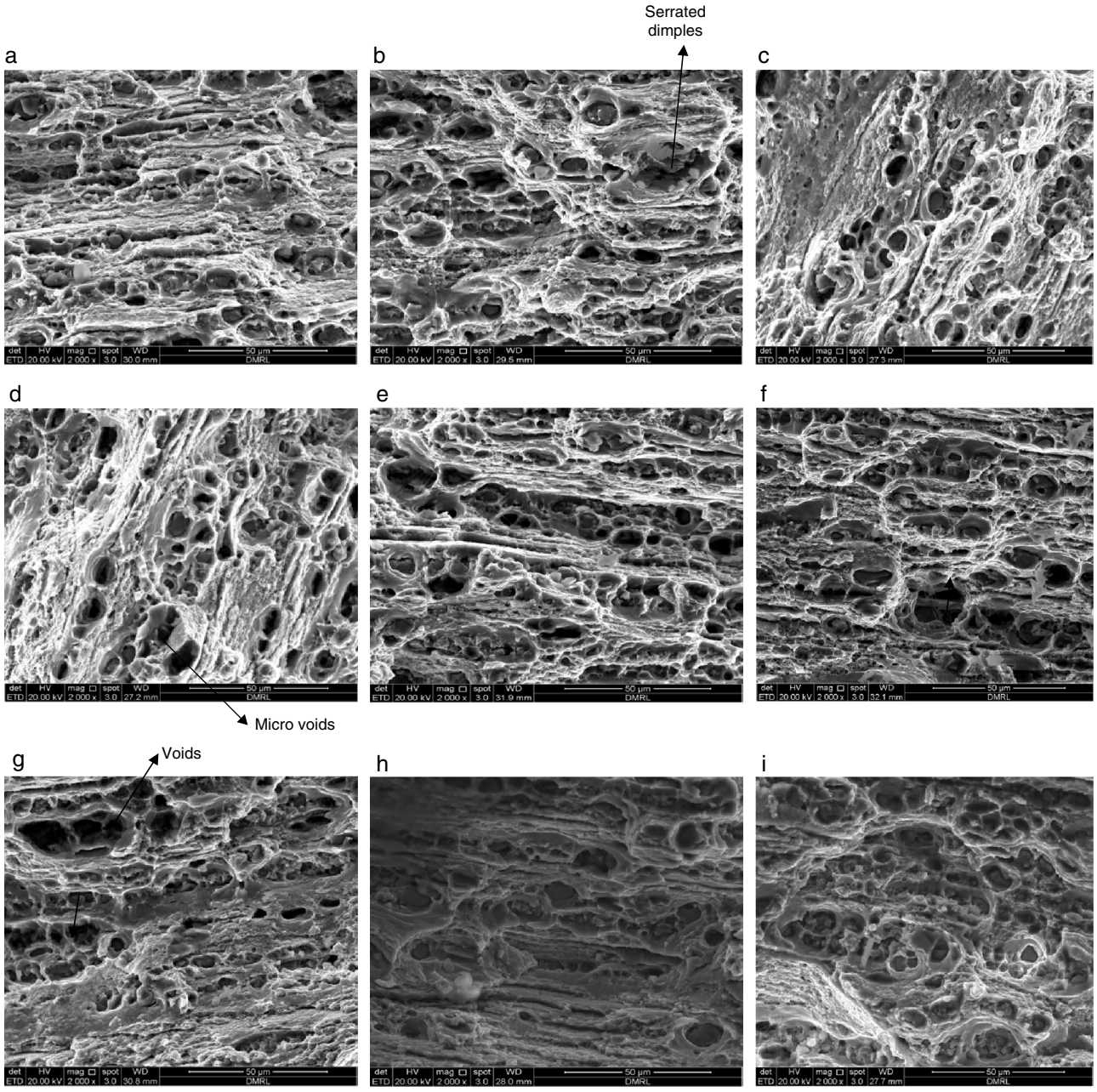

Fig. 7 – SEM micrographs of fracture surface (a) 0.01/s, 20 °C (b) 500/s, 20 °C (c) 1500/s, 20 °C (d) 500/s, 100 °C (e) 1000/s, 100 °C (f) 1500/s, 100 °C (g) 500/s, 300 °C (h) 1000/s, 300 °C (i) 1500/s, 300 °C.

significant at the lower strain rates; where as a more cup- and cone-like surface representing dimple structure is found at the higher strain rates. The dimple structure demonstrates that the material shows ductile fracture. When the load increases, the small dimples collapse and form big dimples. The number of dimples is more at high strain rates than that at quasi-static and intermediate strain rates. The toughness of the material is observed to be more at high strain rates compared to that at low strain rates. The energy absorption of material can be obtained by integrating the true stress with respect to the true strain (Fig. 5 (a)). The aluminium alloy tested in the present study has a maximum energy value of 0.35 J/mm^3 at 1500 s^{-1} strain rate and has a parabolic relation to the true strain. The large energy absorption capacity of the 7017 aluminium is mainly due to its high level of work hardening and large fracture elongation.

The influence of the temperatures on the flow stress curve can be understood in Fig. 5. It is also observed that the flow stress decreases with increase in temperature. The 7017 aluminium alloy demonstrates thermal softening at higher temperatures. So when the temperature is more than 200 °C at these strain rates, thermal softening is predominant mode of deformation mechanism. This softening phenomenon was due to a combination of adiabatic heating, dynamic recovery and dynamic recrystallization. The flow stress softening, which occurred during deformation in the temperature range of (200–300 °C), was caused by the dynamic recovery and adiabatic heating [17].

Fig. 7 depicts the fracture surfaces of tensile specimens at various strain rates and temperatures examined by SEM. From Fig. 7, it is noticed that the fracture surface of 7017 aluminium alloy at low strain rate tensile tests at room temperature consists of the cleavage pattern. However, the fracture plane at high strain rate tests (1500 s^{-1}) at various temperatures is mostly composed of the dimple pattern (Fig. 7), but the number of dimple enhances with rise in temperature from 25 °C to 300 °C. Fig. 7 illustrates that when the temperature increases to 200 °C, the number of dimples rises and the dimple size of 7017 aluminium alloy are larger than that at lower temperature. Failure due to nucleation, growth, and coalescence of microvoids resulting in improvement of ductility [11]. Fig. 7 depicts the pictures of fracture surfaces after high strain rate tensile tests. A small difference in fracture mode is noticed that with decreasing the deformation temperature. The results of comprehensive observations on the central part of the fracture surface are given in Fig. 7. Many dimples with a little cleavage portions on the fracture surfaces tested at high strain rates. The “serrated” dimples become more prominent at lower deformation temperatures. This variation in ductility is also visibly noticeable from Fig. 7. The presence of the Fe-rich and Mn-rich intermetallics at the bottom of the dimples corroborates that the damage initiates from the second-phase particles and damage follows the process of void nucleation, growth and coalescence [14]. Furthermore, it is noted that there are more and more second-phase particles and other precipitates at the bottom of dimples as strain rate increases [18]. The characteristic features of softening ratio, deeper dimples and necking in high strain rate tests represent that the necking development is delayed under dynamic loading due to inertia effect. The amount of necking and damage tend to increase with strain rate. It is also understood that an increased dislocation density is obvious in the dynamic loading condition. Therefore, the larger and deeper dimples also state clearly that dynamic loading leads to the enhancement of ductility of 7017 aluminium alloy. It seems that the plasticity under dynamic loading is enhanced and this phenomenon can be attributed to the dominant softening effect under dynamic deformation. The observed results are similar to the results of Ma et al. [18].

4. Conclusions

This paper has made an attempt to study the high strain rate tensile behaviour of 7017 aluminium alloy at various strain rates and temperatures. The following conclusions are drawn:

- Compared to the low strain rate tension test, the tensile flow stress and failure strain under the high strain rates is higher. The tensile flow stress rises with the increasing of the strain rate.
- The change in fracture mode has been observed at different strain rate loading conditions. A shear mode of fracture is significant at the lower strain rates; where as a more cup- and cone-like surface representing dimple structure is found at the higher strain rates. The number of dimples is more at high strain rates than that at quasi-static and intermediate strain rates. The toughness of the material is observed to be more at high strain rates compared to that at low strain rates.
- It is also observed that the flow stress decreases with increase in temperature. The 7017 aluminium alloy demonstrates thermal softening at higher temperatures. So when the temperature is more than 200 °C at these strain rates, thermal softening is predominant mode of deformation mechanism.
- However, the fracture plane at high strain rate tests (1500 s^{-1}) at various temperatures is mostly composed of the dimple pattern, but the number of dimple enhances with rise in temperature from 25 °C to 300 °C. It is found that when the temperature increases to 200 °C, the number of dimples rises and the dimple size of 7017 aluminium alloy are larger than that at lower temperatures.
- The established J-C model can effectively predict the experimental data over a wider range of temperatures and strain rates.

Conflicts of interest

The authors declare no conflicts of interest.

Acknowledgements

The authors would like to thank Defence Research and Development Organization, India for financial help in carrying out the experiments.

REFERENCES

[1] Jena PK, Jagtap N, Siva Kumar K, Balakrishna Bhat T. Some experimental studies on angle effect in penetration. Int J Impact Eng 2010;37:489–501.

[2] Jena PK, Mishara B, Siva Kumar K, Balakrishna Bhat T. An experimental study on the ballistic impact behavior of some metallic armour materials against 7.62 mm deformable projectile. Mater Des 2010;31:3308–16.

[3] Mondal C, Mishara B, Jena PK, Siva Kumar K, Balakrishna Bhat T. effect of heat treatment on the behavior of an AA7055 aluminum alloy during ballistic impact. Int J Impact Eng 2011;38:745–54.

[4] Mohr D, Gary G, Lundberg B. Evaluation of stress–strain curve estimates in dynamic experiments. Int J Impact Eng 2010;37:161–9.

[5] Oosterkamp LD, Ivankovic A, Venizelos G. High strain rate properties of selected Al-alloys. Mater Sci Eng A 2000;278:225–35.

[6] Smerd R, Winkler S, Salisbury C, Worswick M, Liyod D, Finn M. High strain rate tensile testing of automotive aluminum alloy sheet. Int J Impact Eng 2005;32:541–60.

[7] El-Magd E, Abouridouane A. Characterization, modeling and simulation of deformation and fracture behaviour of the light weight wrought alloys under high strain rate loading. Int J Impact Eng 2006;32:741–58.

[8] Lee WS, Sue WC, Lin CF, Wu CJ. The strain rate and temperature dependence of the dynamic impact properties of 7075 aluminum alloy. J Mater Process Technol 2000;100:116–22.

[9] Lin YC, Xia YC, Chen XM, Chen MS. Constitutive descriptions for hot pressed 2124-T851 aluminum alloy over a wide range of temperature and strain rate. Comput Mater Sci 2010;50:227–33.

[10] Haghdadi N, Zarei-Hanzaki A, Khalesian AR, Abedi HR. Artificial neural network modeling to predict the hot deformation behavior of an A356 aluminum alloy. Mater Des 2013;49:386–91.

[11] Lee W-S, Tang ZC. Relationship between mechanical properties and microstructural response of 6061-T6 aluminum alloy impacted at elevated temperatures. Mater Des 2014;58:116–24.

[12] Pérez-Bergquist SJ, Gray GT, Cerreta EK, Trujillo CP, Pérez-Bergquist A. The dynamic and quasi-static mechanical response of three aluminum armor alloys: 5059, 5083 and 7039. J Mater Sci Eng A 2011;528:8733–41.

[13] Bobbili R, Madhu V, Gogia AK. Neural network modeling to evaluate the dynamic flow stress of high strength armour steels under high strain rate compression. Def. Technol 2014;10(4):334–42.

[14] Porntadawit J, Uthaisangsuk V, Choungthong P. Modeling of flow behavior of Ti–6Al–4V alloy at elevated temperatures. J Mater Sci Eng A 2014;599:212–22.

[15] Johnson GR, Cook WH. Fracture characteristics of three metals subjected to various strains, strain rates, temperatures and pressures. Eng Fract Mech 1985;21: 31–48.

[16] Johnson GR, Cook WH. A constitutive model and data for metals subjected to large strains, high strain rates, and high temperatures. In: Proc. 7th Int. Symp. on Ballistics. The Hague, The Netherlands: The Royal Institution of Engineers in the Netherlands: Division for Military Engineering; 1983. p. 541–7.

[17] Zhou M, Lin YC, Deng J, Jiang Y. Hot tensile deformation behaviors and constitutive model of an Al–Zn–Mg–Cu alloy. Mater Des 2014;59:141–50.

[18] Ma H, Huang L, Tian Y, Li J. Effects of strain rate on dynamic mechanical behavior and microstructure evolution of 5A02-0 aluminum alloy. J Mater Sci Eng A 2014;606:233–9.